

Scaling anomalies in the coarsening dynamics of fractal viscous fingering patterns

Massimo Conti¹, Azi Lipshtat² and Baruch Meerson²

¹*Dipartimento di Matematica e Fisica, Università di Camerino,
and Istituto Nazionale di Fisica della Materia, 62032, Camerino, Italy and*

²*Racah Institute of Physics, Hebrew University of Jerusalem, Jerusalem 91904, Israel*

We analyze a recent experiment of Sharon *et al.* (2003) on the coarsening, due to surface tension, of fractal viscous fingering patterns (FVFPs) grown in a radial Hele-Shaw cell. We argue that an unforced Hele-Shaw model, a natural model for that experiment, belongs to the same universality class as model B of phase ordering. Two series of numerical simulations with model B are performed, with the FVFPs grown in the experiment, and with Diffusion Limited Aggregates, as the initial conditions. We observed Lifshitz-Slyozov scaling $t^{1/3}$ at intermediate distances and very slow convergence to this scaling at small distances. Dynamic scale invariance breaks down at large distances.

PACS numbers: 61.43.Hv, 64.75.+g, 47.54.+r

Coarsening is an important paradigm of emergence of order from disorder. It has been extensively studied in two-phase systems quenched from a disordered state into a region of phase coexistence [1, 2, 3]. In another class of systems, disordered configurations are generated by an instability of growth in combination with noise, and they often exhibit long-range correlations and fractal geometry [4]. Examples include fractal clusters developing in the process of solidification from an under-cooled liquid [5], fractal clusters on a substrate grown by deposition [6] and fractal viscous fingering patterns (FVFPs) formed by the Saffman-Taylor instability in the radial Hele-Shaw cell [5]. When the driving stops, the fractal clusters coarsen by surface tension, and the coarsening dynamics provide a valuable characterization of these systems.

An important simplifying factor in the analysis of coarsening dynamics is *dynamic scale invariance* (DSI): the presence of a *single*, time-dependent length scale $L(t)$, so that a normalized pair correlation function $C(r, t)$ depends, at long times, only on $r/L(t)$. The coarsening length scale $L(t)$ often exhibits a power law in time [3]. For systems with short-range correlations there is a lot of evidence, from experiments and numerical simulations, in favor of DSI [3]. For systems with long-range correlations the situation is more complicated. In the case of a non-conserved order parameter DSI was established in particle simulations following a quench from $T = T_c$ to $T = 0$ [7]. Implications of mass conservation in DSI were addressed more recently, in the context of coarsening of fractal clusters. Most remarkable of them is the predicted decrease of the cluster radius with time [8]. As of present, only the systems where the conservation law is imposed *globally*, rather than locally, have been found to indeed show this effect [9]. On the contrary, the “frozen” structure of fractal clusters at large distances, observed in simulations of *locally* conserved (diffusion-controlled) fractal coarsening [10, 11, 12, 13] implies breakdown of DSI in these systems [11, 13]. The frozen structure is

due to Laplacian screening of transport at large distances [13].

An additional scaling anomaly, observed in the numerical simulations of diffusion-controlled fractal coarsening [10, 11, 12, 13], was the presence of *two* apparently different dynamic length scales. For one of them, determined from the time-dependence of either the slope of the Porod-law part of $C(r)$ [11, 12, 13], or the cluster perimeter [10, 11, 13], a power law in time was reported: $L_1 \sim t^{0.20-0.23}$. Another length scale, determined from a knee-like structure in $C(r)$ at moderate distances behaves like $L_2 \sim t^{0.30-0.32}$ [13]. While $L_2(t)$ can be identified as Lifshitz-Slyozov length scale $\sim t^{1/3}$ [13], the length scale $L_1(t)$ looks unusual.

Strikingly similar results were recently obtained in experiment on the coarsening dynamics of a *different* system: radially grown FVFPs in a Hele-Shaw cell [14]. The frozen structure at large distances, observed in Ref. [14], clearly indicates breakdown of DSI. Furthermore, two different time-dependent length scales, with apparent dynamic exponents 0.22 and 0.31, are observed [14]. Why is this system so similar to the diffusion-controlled system? Where does the exponent 0.20 – 0.23 come from? These questions are addressed in the present work. We first suggest an unforced Hele-Shaw model and discuss its properties. A scaling argument indicates that this model belongs to the same universality class as the so called model B, the standard model of the diffusion-controlled phase separation in two-phase systems [3]. Assuming universality, we performed a series of numerical simulations with model B, where the FVFPs, grown in experiment of Sharon *et al.* [14], are used as the initial conditions for the minority phase. Then we report additional simulations of fractal coarsening, with DLAs (Diffusion Limited Aggregates) as the initial conditions. These two series of simulations show Lifshitz-Slyozov scaling $t^{1/3}$ at intermediate distances. Breakdown of dynamic scale invariance at large distances is confirmed. However, the existence of an anomalous power law in $L_1(t)$ is disproved.

A natural description of coarsening of FVFPs is provided in terms of an unforced Hele-Shaw (UHS) flow. Consider a Hele-Shaw flow [15] and assume that the driving fluid (for example, air) has negligible viscosity, so that the pressure inside it is spatially uniform. When the plate spacing b is very small, the flow is effectively two-dimensional, and the velocity of the viscous fluid (for example, oil) is $\mathbf{v}(\mathbf{r}, t) = -(b^2/12\mu)\nabla p(\mathbf{r}, t)$, where p is the pressure and μ is the dynamic viscosity of the driven fluid. As the fluids are immiscible, the interface speed is

$$v_n = -\frac{b^2}{12\mu}\nabla_n p, \quad (1)$$

where index n denotes the components of the vectors normal to the interface, and the gradient is evaluated at the respective points of the interface γ . Assuming incompressibility of the driven fluid, $\nabla \cdot \mathbf{v} = 0$, one arrives at Laplace's equation for the pressure:

$$\nabla^2 p = 0. \quad (2)$$

The pressure jump across the interface is [16]

$$\Delta p = \frac{\sigma}{b} \left[1 + 3.8 \left(\frac{\mu v_n}{\sigma} \right)^{2/3} \right] + \frac{\pi}{4} \sigma \mathcal{K}, \quad (3)$$

where σ is surface tension, and \mathcal{K} is the curvature of the interface. At the coarsening stage the interface speed is very small, so the second term in the square brackets can be neglected. The first term does not depend on the coordinates, so one arrives at a Gibbs-Thomson relation

$$\Delta p = \frac{\pi}{4} \sigma \mathcal{K}. \quad (4)$$

To close this set of equations, one more condition is needed. A natural condition to demand during the *growth* stage is a constant-in-time driving pressure [17], or a constant areal flow rate of the driving fluid. Each of these conditions assumes evacuation of the driven fluid at the external boundary of the system. In the coarsening problem both the supply of the driving fluid, and evacuation of the driven fluid are blocked. Therefore, the normal component of the velocity of the driven fluid at the external boundary Γ should vanish, which follows

$$\nabla_n p|_{\Gamma} = 0. \quad (5)$$

Equations (1), (2), (4) and (5) define a one-sided version of the UHS model. Similar models have been used in the context of break-ups (pinch-offs) of bubbles, driven only by surface tension [18, 19]. The UHS model has two important properties: (i) The total area A of the driving fluid is constant. (ii) The total length of the interface is a non-increasing function of time [20].

Now let us compare the UHS model with model B, the phase-field formulation of which is given by the Cahn-Hilliard equation for the order parameter $u(\mathbf{r}, t)$ [3]:

$$\frac{\partial u}{\partial t} + \frac{1}{2} \nabla^2 (\nabla^2 u + u - u^3) = 0. \quad (6)$$

At late times, the two-phase dynamics are describable by an asymptotic sharp-interface theory [21]. In the sharp-interface limit, the interface speed is

$$v_n = \frac{1}{4} (-\nabla_n \Phi^{out} + \nabla_n \Phi^{in}), \quad (7)$$

where potential $\Phi(\mathbf{r}, t)$ is a harmonic function in each of the two phases *in* and *out*. The boundary conditions are $\Phi|_{\gamma} = (\sqrt{2}/3)\mathcal{K}$ and $\nabla_n \Phi|_{\Gamma} = 0$.

How are these two problems related? To begin with, the sharp-interface limit of model B has the same properties (i) and (ii) as the UHS model [21], so each of the two models describes interface-shortening dynamics under area conservation. The models do differ from each other considerably in the *final* outcomes of the coarsening dynamics. For a steady state solution of the UHS model one has simply $p = const$. Therefore, possible stationary shapes of domains of the driving fluid in the UHS model are *one or more* circular bubbles of arbitrary radii. On the contrary, in model B, $\Phi = const$ cannot be a steady state solution in the presence of more than one bubbles, because it cannot obey all the boundary conditions on the multiple interfaces. Therefore, a generic final state here is always a *single* circular bubble. In model B bubbles compete for material via diffusion through the majority phase. Obviously, this competition mechanism (Ostwald ripening [2, 3]) is absent in the UHS model.

This difference between the two models becomes crucial after the driving fluid breaks up into multiple bubbles. Before it happens, the two models can be expected to behave similarly. A simple argument for this follows from scaling analysis. Consider coarsening of a domain of complex shape and assume for a moment DSI, that is a *single* relevant length scale $L = L(t)$. The pressure jump across the interface can be estimated from Eq. (4): $\Delta p \sim \sigma/L$. Then, from Eq. (1), $v_n \sim b^2\sigma/(\mu L^2)$. On the other hand, $v_n \sim \dot{L}$. This yields a coarsening law $L(t) \sim (b^2\sigma t/\mu)^{1/3}$. We checked that this estimate is in excellent agreement with the experimental result [14] for $L_2(t)$, for two latest decades of time.

The same power law $t^{1/3}$ is obtained in model B [2, 3]. Therefore, if DSI holds, the two models belong to the same universality class. In reality, each of these two systems exhibits breakdown of DSI at large distances, when one deals with fractal clusters at $t = 0$ [11, 12, 13, 14]. At intermediate distances, however, the classic exponent $1/3$ is observed in both systems [13, 14]. Therefore, we conjecture that, prior to major breakup, the two models belong to the same universality class.

Based on this conjecture, we performed two series of simulations with model B [Eq. (6)]. Details of our numerical procedure and diagnostics can be found in Refs. [11, 13]. In the first series of simulations we used FVFPs grown in experiment [14] as the initial conditions for the "minority phase" $u = 1$. The fractal dimension of these patterns, determined from the pair correlation

function, is close to 1.71. The (scaled) system size was 1024×1024 , with periodic boundary conditions. The (scaled) time range of the simulations was $0 < t < 3 \cdot 10^4$. Figure 1 shows snapshots of the simulated coarsening dynamics. The snapshots closely resemble those observed in experiment [14]. Figure 2 presents the (normalized) equal-time pair correlation function $C(r, t)$ at different times, and the characteristic dynamic length scales. The data is averaged over 7 simulations with different FVFPs. $C(r, t)$ in a linear scale is shown in Fig. 2a. At small distances C goes down linearly with r (the Porod law) [3], and the inverse slope of this linear dependence yields the “coarsening length scale” $L_1(t)$ depicted in Fig. 2d. The log-log plots of $C(r, t)$ (Fig. 2b) indicate an invariable fractal dimension of the cluster at large distances (up to the upper cutoff of the fractal). In addition, Fig. 2b exhibits a knee-like feature. In the previous work [13] a similar knee-like feature served to identify Lifshitz-Slyozov length scale $L_2(t)$. Here, following Sharon *et al.* [14], we subtracted from $C(r, t)$ its initial value $C(r, 0)$, and followed the dynamics of the difference, see Fig. 2c. The knee-like feature of Fig. 2b becomes here a local minimum whose position at different times yield a sharp estimate of $L_2(t)$. The “frozen” tail at the distances much larger than $L_2(t)$, but still much smaller than the system size, implies breakdown of DSI.

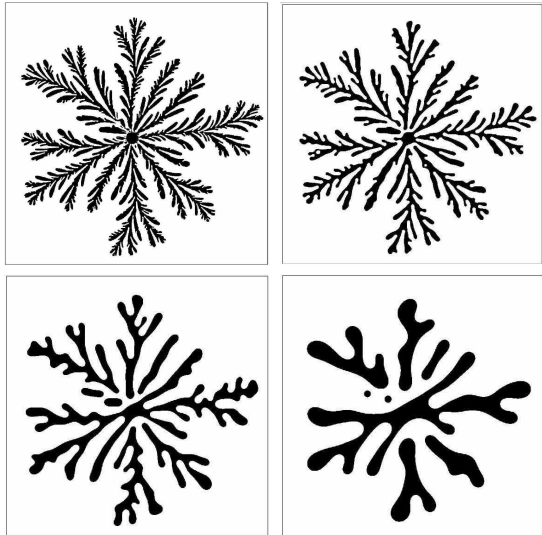


FIG. 1: Snapshots of coarsening of FVFPs simulated with model B. The upper left figure ($t = 0$) shows a FVFP ($D \simeq 1.71$) grown in experiment [14]. The rest of the snapshots show the simulation results at scaled times $t = 290$ (upper right), 3817 (lower left) and 30000 (lower right).

Power-law fits of the data shown in Fig 2d yield the following dynamic exponents: $\alpha_1 = 0.24 \pm 0.01$ for $L_1 \sim t^{\alpha_1}$ and $\alpha_2 = 0.30 \pm 0.01$ for $L_2 \sim t^{\alpha_2}$. The same result for α_1 is obtained from a power-law fit of the cluster perimeter versus time $P(t) \sim t^{-\alpha_1}$, as expected [3, 9, 10, 11, 13]. While the value of α_2 is very close to that obtained

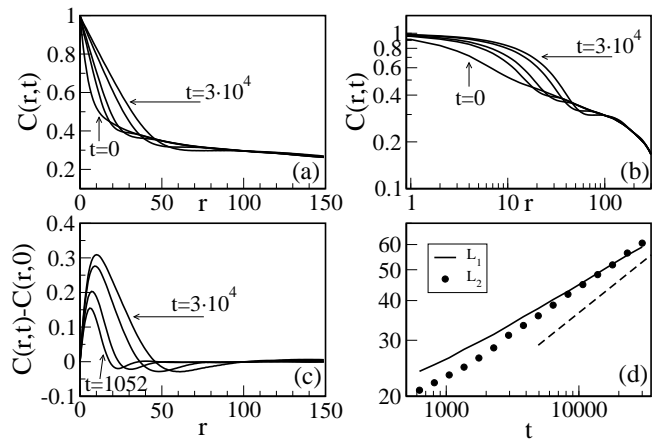


FIG. 2: The dynamics of the equal-time pair correlation function $C(r, t)$ (a-c), and the dynamic length scales $L_1(t)$ and $L_2(t)$ (d) from simulations with model B. The initial conditions are the FVFPs grown in experiment [14]. The time moments are $t = 0$ (figures a and b only), 1052, 2950, 13846 and $3 \cdot 10^4$. The dashed line describes a power law $\sim t^{1/3}$ and is shown here to guide the eye. See text for further details.

in earlier simulations of model B [13] and experiment with the FVFPs [14], $\alpha_1 = 0.24$ is somewhat larger than the values 0.20 – 0.23 reported earlier for these two systems [10, 11, 12, 13, 14]. Also, noticeable in Fig. 4d is curvature of the log-log plot of $L_1(t)$. These observations put forward a question about the true asymptotic value of exponent α_1 .

To address this question, we performed a series of larger simulations, extending the time interval until $t = 10^5$ (which is 20 times longer than the first phase-field simulations of this system [11]). The initial conditions for the minority phase were DLA clusters, “reinforced” by an addition of peripheral sites. The clusters occupied the 1024×1024 box; they had a larger fractal range than the FVFPs grown in experiment [14]. Figure 3 shows snapshots of the simulated coarsening dynamics. Figure 4a presents $C(r, t)$ averaged over 6 different realizations of DLA. Again, following some initial “evaporation” of the minority phase (which happens at an earlier stage of the Cahn-Hilliard dynamics), the tail of $C(r)$ is frozen until very long times. The dynamic length scale $L_2(t)$ is shown in Fig. 4b; a power law fit at long times yields $\alpha = 0.31 - 0.32$ which is close to $1/3$, as expected. The cluster perimeter versus time is shown in Fig. 4c. It can be seen that $P(t)$ has not approached yet a power law. Therefore, we followed Huse [22] and introduced an effective *time-dependent* exponent $-\alpha_1(t)$ which is shown in Fig. 4d versus the perimeter P itself. An asymptotic value of $-\alpha_1(t)$ is obtained by linear extrapolation $t \rightarrow \infty$, that is $P \rightarrow 0$. This procedure yields $\alpha_1 = 0.34$, very close to $1/3$.

Overall, our simulations with model B are in remarkable agreement with experiment on the Hele-Shaw coars-

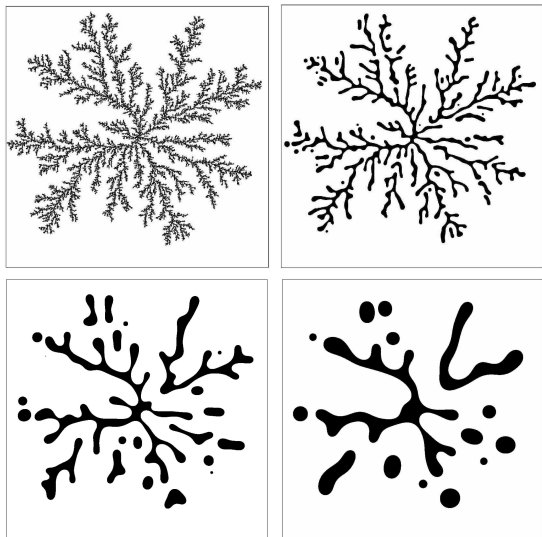


FIG. 3: Snapshots of coarsening of DLA clusters ($D \simeq 1.71$), simulated with model B, at scaled times $t = 0$ (upper left), 1350 (upper right), 26591 (lower left) and 10^5 (lower right).

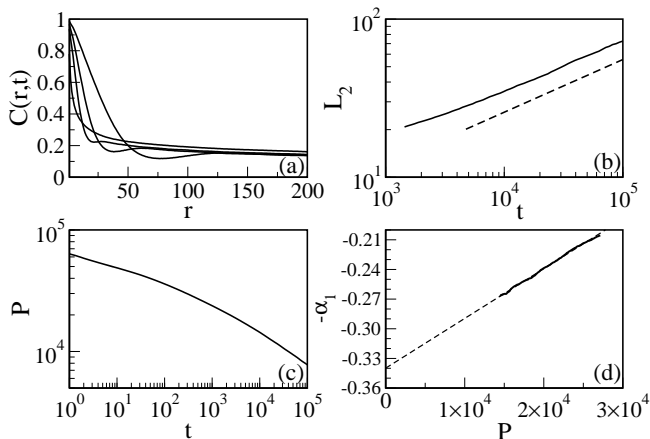


FIG. 4: $C(r, t)$ at $t = 0, 1026, 10521$ and 10^5 (a), $L_2(t)$ (b) and $P(t)$ (c). The dashed line describes a power law $\sim t^{1/3}$ and is shown here to guide the eye. The effective time-dependent exponent α_1 versus P is shown in Fig. d. Linear extrapolation to $P = 0$ (dashed line) yields $\alpha_1 = 0.34$.

ening of FVFPs [14]. Breakdown of DSI at large distances and the Lifshitz-Slyozov scaling $t^{1/3}$ at intermediate distances are firmly established. Our simulations show, however, that the “unusual” dynamic exponent $0.20 - 0.23$ is a transient on the way to $1/3$. This finding explains the apparent independence of the unusual exponent on the fractal dimension of the cluster, observed in Ref. [13]. In view of the conjectured universality, we expect that the same kind of behavior will be observed in a larger-scale experiment on the coarsening of FVFPs, and in direct simulations with the unforced Hele-Shaw model.

We are grateful to Eran Sharon and his colleagues for

providing images of FVFPs, that were used in our simulations, and for useful discussions. We thank Avner Peleg and Boris Zaltzman for advice. The work was supported by the Israel Science Foundation (grant No. 180/02).

-
- [1] I.M. Lifshitz, Zh. Eksp. Teor. Fiz. **42**, 1354 (1962) [Engl. Transl., Sov. Phys. JETP **15**, 939 (1962)].
- [2] I.M. Lifshitz and V.V. Slyozov, J. Phys. Chem. Solids **19**, 35 (1961).
- [3] J.D. Gunton, M. San Miguel, and P.S. Sahni, in *Phase Transitions and Critical Phenomena*, edited by C. Domb and J.L. Lebowitz (Academic Press, New York, 1983), Vol. 8, p. 267; A.J. Bray, Adv. Phys. **43**, 357 (1994).
- [4] J. Feder, *Fractals* (Plenum, New York, 1988); T. Vicsek, *Fractal Growth Phenomena* (World Scientific, Singapore, 1992); P. Meakin, *Fractals, Scaling and Growth Far from Equilibrium* (Cambridge University Press, Cambridge, 1997).
- [5] J.S. Langer, Rev. Mod. Phys. **52**, 1 (1980).
- [6] C. Bréchnignac *et al.*, Phys. Rev. Lett. **88**, 196103 (2002).
- [7] K. Humayun and A.J. Bray, J. Phys. A **24**, 1915 (1991); Phys. Rev. B **46** 10594 (1992).
- [8] R. Sempéré *et al.*, Phys. Rev. Lett. **71**, 3307 (1993); B. Meerson and P.V. Sasorov, e-print cond-mat/9708036.
- [9] A. Peleg, M. Conti and B. Meerson, Phys. Rev. E **64**, 036127 (2001).
- [10] T. Irisawa, M. Uwaha and Y. Saito, Europhys. Lett. **30**, 139 (1995).
- [11] M. Conti, B. Meerson and P.V. Sasorov, Phys. Rev. Lett. **80**, 4693 (1998).
- [12] S.V. Kalinin *et al.*, Phys. Rev. E **61**, 1189 (2000).
- [13] A. Lipshtat, B. Meerson and P.V. Sasorov, Phys. Rev. E **65**, 50501(R) (2002).
- [14] E. Sharon, M.G. Moore, W.D. McCormick, and H.L. Swinney, Phys. Rev. Lett. **91**, 205504 (2003).
- [15] P.G. Saffman and G.I. Taylor, Proc. Roy. Soc. London, Ser. A **245**, 312 (1958).
- [16] C.-W. Park and G.M. Homsy, J. Fluid Mech. **139**, 291 (1984).
- [17] D. Bensimon *et al.*, Rev. Mod. Phys. **58**, 977 (1986).
- [18] R. Almgren, Phys. Fluids **8**, 344 (1996).
- [19] (i) Notice that $\nabla^2 p$ is non-zero inside bubbles of compressible fluid until all bubbles reach their final (circular) shapes. Therefore, while the total area of all bubbles is conserved in the process of relaxation, the areas of individual bubbles are not. (ii) After breakup the pressure inside each bubble must be specified uniquely. In a simplified description $p|_{\gamma_i} = p_i^{(0)} A_i^{(0)} / A_i(t) + (\pi/4) \sigma \mathcal{K}$ at each bubble interface γ_i . Here $A_i(t)$ is the area of the i -th bubble, and $A_i^{(0)}$ and $p_i^{(0)}$ are the bubble area and air pressure at the time of creation of the bubble. Here we assume that, after a break-up event, the pressures in each of the two new bubbles are equal. (iii) If the driving fluid is incompressible, then $\nabla^2 p = 0$ inside it, and one can safely put $p|_{\gamma_i} = (\pi/4) \sigma \mathcal{K}$. Of course, in the latter case the dynamics preserve the area of each bubble.
- [20] For a single bubble, these two properties were proved by P. Constantin and M. Pugh, Nonlinearity **6**, 393 (1993).
- [21] R.L. Pego, Proc. R. Soc. Lond. A **422**, 261 (1989).
- [22] D.A. Huse, Phys. Rev. B **34**, 7845 (1986).